Influence of Indenyl Ligand Substitution Pattern on Metallocene-Catalyzed Ethene Copolymerization with 1-Octene

Martin Julius Schneider,[†] Jürgen Suhm,[†] Rolf Mülhaupt,*[,†] Marc-Heinrich Prosenc,[‡] and Hans-Herbert Brintzinger[‡]

Freiburger Materialforschungszentrum und Institut für Makromolekulare Chemie, Albert-Ludwigs-Universität Freiburg, Stefan-Meier-Strasse 21, D-79104 Freiburg i.Br., Germany, and Fakultät für Chemie, Universität Konstanz, D-78434 Konstanz, Germany

Received December 16, 1996; Revised Manuscript Received March 31, 1997[⊗]

ABSTRACT: The influence of silylene-bridged bis(indenyl) ligand substitution, especially benzannelation and 2-methyl substitution, on methylaluminoxane-activated metallocene-catalyzed ethene/1-octene copolymerization in toluene at 40 °C was investigated. 2-Methyl substitution gave significantly higher molecular masses at the expense of catalyst activity, whereas benzannelation promoted 1-octene incorporation and randomness of the resulting poly(ethene-*co*-1-octene) copolymers. Force field calculations based on steric arguments were used to explain experimental copolymerization results. Activation energy differences between ethene and 1-octene insertion accounted for improved 1-octene incorporation in the case of benzannelated metallocenes. According to ^{13}C-NMR microstructure analysis, copolymerization followed first-order Markov statistics.

Introduction

In contrast to conventional multisite Ziegler−Natta catalysts, single-site metallocene-based catalysts produce very uniform homo- and copolymers. As a function of metallocene structure, it is possible to control stereochemistry, molecular mass, end groups, and short-chain branching without affecting narrow molecular mass distributions of $M_w/M_n = 2$.[1−3] One attraction of the metallocene-catalyzed ethene copolymerization is incorporation of 1-olefin comonomers into the polyethene backbone over the entire feasible composition range from 0 to 100% comonomer content. Moreover, metallocene-based catalysts also incorporate cycloolefins, styrene, and higher 1-olefins, which were difficult to copolymerize with most conventional catalysts.[4−9] Comonomer incorporation is independent of copolymer molecular mass, whereas early generations of Ziegler−Natta catalysts, possessing different catalytically active centers, frequently incorporate larger amounts of 1-olefin comonomer in low molecular mass fractions. Metallocene-catalyzed copolymerization represents a versatile synthetic route to families of tailor made polymeric materials, ranging from low and very low density polyethylenes to amorphous high-T_g cycloolefin copolymers, rubbers, thermoplastic elastomers, and flexible polyolefins which are of interest as blend components and toughening agents.

In stereo- and regioselective metallocene-catalyzed propene polymerization, steric control depends primarily on metallocene structure, especially metallocene symmetry. Only C_2- and some C_1-symmetrical ansa-metallocenes produce isotactic polypropene, whereas C_s-symmetrical metallocenes form either atactic or syndiotactic polypropenes.[1−3] Molecular mass is dependent on metallocene structure. Brintzinger[10] and Spaleck[11−13] have discovered almost simultaneously that benzannelation and especially 2-methyl substitution of silylene-bridged bis(indenyl) zirconocenes leads to a substantial increase in molecular masses. Several investigations concerning the influence of metallocene structures in ethene copolymerization were made.[14−18] Syndiospecific metallocenes, used to produce syndiotactic polypropenes, are reported to promote ethene copolymerization with higher 1-olefins. Metallocene structure is the key for controlled comonomer incoporation.

The purpose of this research was to examine the effect of ligand substitution pattern, especially of benzannelation and 2-methyl substitution, on methylaluminoxane (MAO)-activated $Me_2Si(Ind)_2ZrCl_2$ ethene/1-octene copolymerization. Many experimental data available about comonomer incorporation stand in contrast to the lack of mechanisms and regulation factors for the reasons of comonomer incorporation. Therefore, we wish to report a force field calculation that is able to support the experimental copolymerization behavior of the substituted silylene-bridged bis(indenyl) ligands in ethene/1-octene copolymerization.

Experimental Section

Materials. *rac*-$Me_2Si(Ind)_2ZrCl_2$ abbreviated as I, *rac*-$Me_2Si(2\text{-MeInd})_2ZrCl_2$ abbreviated as MI, *rac*-$Me_2Si(Benz[e]\text{-}Ind)_2ZrCl_2$ abbreviated as BI, and *rac*-$Me_2Si(2\text{-MeBenz}[e]\text{-}Ind)_2ZrCl_2$ abbreviated as MBI (see Figure 2) were obtained from Dr. Udo Stehling of Prof. Brintzinger's group who is gratefully acknowledged. 1-Octene was obtained from Aldrich Co., MAO (10 wt % in toluene, $M_n = 1000$ g/mol) from Witco Germany, toluene from Roth GmbH, and ethene from Gerling Holz u. Co., Handels-GmbH, Hamburg. Toluene solvent was rectified over $LiAlH_4$ and refluxed and distilled over Na/K alloy prior to use. 1-Octene was distilled over CaH_2. Metallocenes, ethene, and MAO were used without further purification. All catalyst components, including toluene solvent and monomers, were handled and stored under a dry argon atmosphere.

Polymerization. Polymerization reactions were performed in a glass reactor rinsed with 150 mL of a 0.03 mol/L $Al(iBu)_3$ solution in toluene prior to use. Typically, 86.3 mL of toluene, 9.2 mL of 1-octene, and 2.5 mL of MAO solution were pumped into the glass reactor. The total volume of the reaction mixture was 100 mL at all polymerization temperatures. After thermal equilibration of the reactor system, ethene was continuously added by a mass flow meter (F-111C, Bronkhorst, Nl-7261 AK Ruurlo, Netherlands) until the reaction mixture was saturated with ethene. The polymerization was started by adding 0.2 μmol of one metallocene in 2 mL of toluene, equivalent to [Zr] = 2.0 μmol/L and [Al] = 40 mmol/L. The pressure of ethene was kept constant at 2 bar during the polymerization, and the

[†] Albert-Ludwigs-Universität Frieburg.
[‡] Universität Konstanz.
[⊗] Abstract published in *Advance ACS Abstracts,* May 1, 1997.

S0024-9297(96)01844-X CCC: $14.00

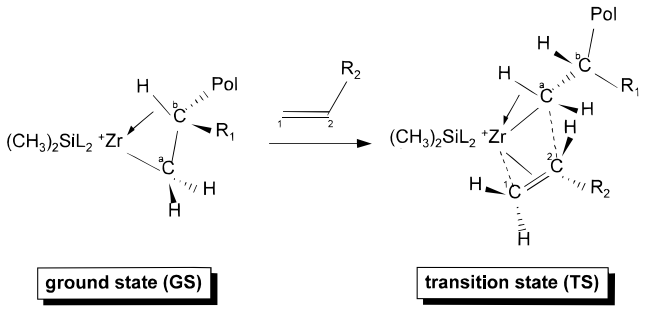

Figure 1. Ground (GS) and transition states (TS) used for force field calculations (L = different indenyl ligands (see Figure 2); R_1, R_2 see Tables 1 and 2).

Table 1. Ground States Used for Force Field Calculations

R_1[a]	LIM[b]	abbreviation
−H	ethene	GS(E-Pol)
$-C_6H_{13}$	1-octene	GS(O-Pol)

[a] R_1 at ground state (GS); see Figure 1. [b] LIM = last inserted monomer unit at ground state (GS).

Table 2. Transition States Used for Force Field Calculations

R_1[a]	LIM[b]	R_2[a]	COM[c]	abbreviation
−H	ethene	−H	ethene	TS(M_E, E-Pol)
−H	ethene	$-C_6H_{13}$	1-octene	TS(M_O, E-Pol)
$-C_6H_{13}$	1-octene	−H	ethene	TS(M_E, O-Pol)
$-C_6H_{13}$	1-octene	$-C_6H_{13}$	1-octene	TS(M_O, O-Pol)

[a] R_1, R_2 at transition state (TS); see Figure 1. [b] LIM = last inserted monomer unit at transition state (TS). [c] COM = coordinated monomer at transition state (TS).

vapor pressure of the solvent was considered when the ethene concentration was calculated.

Copolymerizations were performed to afford low conversions. Typically, after 10 min copolymerization was quenched by adding 10 mL of 2-propanol. The copolymer produced was precipitated in 300 mL of methanol acidified with 10 mL of 10 wt % aqueous HCl, filtered, and dried at 60 °C under vacuum.

Characterization. ^{1}H-NMR spectra were recorded from solutions of 80 mg of polymer in 0.5 mL of $CDCl_3$ at room temperature by a Bruker ARX 300 at 300 MHz; ^{13}C-NMR spectra, at 75.4 MHz, with a 30° pulse angle, 2 s delay, and at least 8000 scans. The signals were referenced to the methyl signal (δ = 14.84 ppm) of the poly(ethene-*co*-1-octene). Size exclusion chromatographic (SEC) analyses of molecular mass and molecular mass distribution were performed at BASF AG. Glass temperatures were determined by means of differential scanning calorimetry (DSC) with a Perkin-Elmer Series 7 from the heating curve at a heating rate of 20 K/min after twice previous cooling to −150 °C with 20 K/min and heating to 0 °C with 20 K/min.

We have used the equations reported by Randall[19] to calculate the monomer sequence distribution. We calculated the *r* parameters by assuming a first-order Markov statistics and minimized the differences between the monomer sequence distribution determind by ^{13}C-NMR and the simulated monomer sequence distribution.[4]

Force Field Calculations. We calculated activation energies as energy differences between assumed ground (GS) and transition states (TS) by varing the last inserted monomer unit (ethene or 1-octene) in the case of the ground state and the coordinated monomers and the last inserted monomer units in the case of the transition state for the four used metallocenes (see Figure 1 and Tables 1 and 2). The structure of the ground state was taken from the reported X-ray structure of the model compound $[(C_5H_4Me)_2Zr(CH_2CH_3)(PMe_3)][BPh_4]$,[20] with a stable β-agostic hydrogen bond. The structure of the transition state was assumed to be similar to the calculated transition state reported by Woo, Fan, and Ziegler.[21]

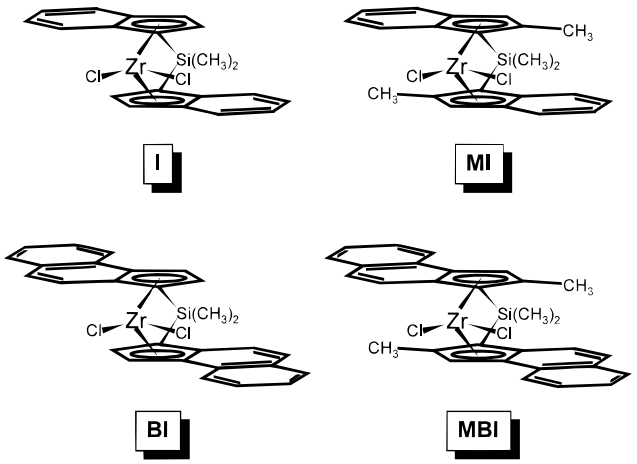

Figure 2. Benzannelated and 2-methyl-substituted $Me_2Si(Ind)_2ZrCl_2$ metallocene familiy (I, indenyl; B, benzannelation; M, 2-methyl substitution).

Table 3. Results of Copolymerizations of Ethene and 1-Octene Using Different Metallocenes[a]

	metallocene (run no.)			
	I (1)	MI (2)	BI (3)	MBI (4)
ethene content[b] (mol %)	88.2	88.6	80.6	77.8
1-octene content[b] (mol %)	11.8	11.4	19.4	22.2
ethene content[b] (mol %)	65.1	65.9	50.9	46.7
1-octene content[b] (mol %)	34.9	34.1	49.1	53.3
r_E	18.9	19.5	10.7	10.1
r_O	0.014	0.013	0.076	0.118
$r_E r_O$	0.27	0.25	0.81	1.20
activity[c]	1 598 000	894 000	1 667 000	596 000
M_n[d] (g/mol)	90 800	140 000	77 700	172 000
M_w/M_n[d]	1.6	1.8	1.6	1.8
P_n[e]	2390	3720	1750	3690
T_g[f] (°C)	−48.9	−45.9	−57.1	−58.5

[a] P_E = 2 bar, [E] = 0.2 mol/L = 25 mol %, [O] = 0.6 mol/L = 75 mol %, [Zr] = 2 μmol/L, [Al] = 40 mmol/L, [Al]/[Zr] = 20 000, 40 °C, solvent toluene. [b] Determined by ^{13}C-NMR. [c] $[(mol_{\text{inserted monomer units}})/(mol/L_{\text{total monomer conc}} \times mol_{\text{metallocene}} \times h_{\text{polymerization time}})]$. [d] Determined by GPC using polystyrene standards. [e] Degree of polymerization. [f] Determined by DSC, heating rate 20 K/min.

For force field calculations (Biosym Software: forcefield "Discover", parameter set[22]) we fixed the positions of the metal center and the nearest atoms (Figure 2: ^{a}C, ^{b}C, ^{1}C, ^{2}C, and the directly bonded atoms) to retain the structure of the catalytic center.

Results and Discussion

For a study of the effects of benzannelation and 2-methyl substitution in ethene copolymerization, ethene/1-octene (1 mol/3 mol) was copolymerized in toluene at 40 °C in the presence of 2 μmol/L zirconocenes, as displayed in Figure 2, which were activated with methylaluminoxane (MAO) using [Al] = 40 mmol/L and [Al]/[Zr] = 20 000. High 1-octene content was used to examine the influence of high comonomer content and to assure that both catalyst and copolymer remain in toluene solution during copolymerization. Moreover, ethene copolymers with a 1-octene content higher than 20 wt % are of interest as elastomers and blend components.[9]

In Table 3, incorporation of 1-octene, catalyst activity, molecular mass, molecular mass distribution, degree of polymerization, and copolymerization parameters as well as $r_O r_E$, which is an indicator for randomness of the copolymers, are listed as a function of metallocene indenyl ligand substitution. For better comparison of

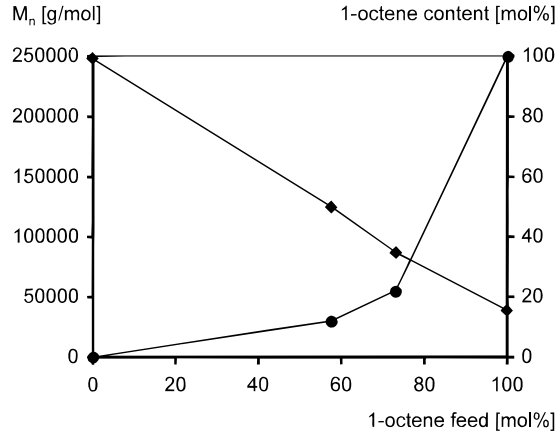

Figure 3. Molecular mass and 1-octene content of poly(ethene-*co*-1-octene) as a function of 1-octene feed.

the copolymerization involving ethene and 1-octene, the catalyst activity was not referred to the mass of the resulting copolymer, but to the number of inserted monomers, which is calculated from polymerization yield and comonomer content. Clearly, 2-methyl substitution of indenyl as well as the benz(*e*)indenyl ligand caused reduced catalyst activity and promoted formation of higher molecular mass copolymers without affecting the narrow molecular mass distribution, which remained $M_w/M_n = 1.8$, independent of metallocene structure. In the series I and BI, benzannelation reduced molecular masses, whereas benzannelation of the 2-methyl-substituted metallocenes (cf. MI versus MBI, Table 3), slightly improved the molecular mass. When degrees of polymerization (P_n in Table 3) are compared, benzannelation of the indenyl ligand accounts for a much larger decay than benzannelation of the 2-methyl-substituted indenyl ligand.

According to ^{1}H-NMR studies, only vinylidene-type end groups, corresponding to the NMR signal at $\delta =$ 4.65 ppm and resulting from β-hydride elimination after insertion of 1-octene, are visible. This is an indication that chain termination occurred exclusively after insertion of 1-octene. The reinsertion of the vinylidene-type end groups could not be detected when these metallocene catalysts were used.

Table 4. Results of Homo- and Copolymerizations of Ethene and 1-Octene Using MBI

	run 5	run 4	run 6	run 7
ethene conc (mol %)	0	25	40	100
1-octene conc (mol %)	100	75	60	0
ethene conc (mol/L)	0.0	0.2	0.2	0.2
1-octene conc (mol/L)	1.3	0.6	0.3	0.0
total monom conc (mol/L)	1.3	0.8	0.5	0.2
MBI conc (μmol/L)	40	2	2	2
Al conc (μmol/L)	80	40	40	40
ethene content[a] (mol %)	0.0	77.8	88.0	100.0
1-octene content conc (μmol/L)	100.0	22.2	12.0	0.0
ethene content[a] [Gew.%]	0.0	46.7	64.7	100.0
1-octene content[a] [Gew.%]	100.0	53.3	35.3	0.0
r_E		10.1	10.6	
r_O		0.118	0.114	
$r_E r_O$		1.20	1.20	
activity[b]	840	596 000	1 404 000	6 214 000
M_n[c] (g/mol)	39 000	87 000	125 000	248 000
M_w/M_n[c]	1.7	2.2	2.0	2.7
P_n[d]	350	1.870	3.280	8.860
T_g[e] (°C)	−62.7	−58.5	−45.8	−80.0

[a] Determined by ^{13}C-NMR. [b] $[(\text{mol}_{\text{inserted monomer units}})/(\text{mol/L}_{\text{total monomer conc}} \times \text{mol}_{\text{metallocene}} \times \text{h}_{\text{polymerization time}})]$. [c] Determined by GPC using polyethylene standards. [d] Degree of polymerization. [e] Determined by DSC, heating rate 20 K/min.

The degree of polymerization decreased with increasing 1-octene incorporation, which was promoted by benzannelation. As is apparent in Table 3, at an ethene/1-octene 1 mol/3 mol molar ratio, 2-methyl substitution did not affect 1-octene incorporation, whereas benzannelation of both indenyl and 2-methyl-substituted indenyl ligands almost doubles the molar content of 1-octene. When I and MI or BI and MBI are compared, the 1-octene content of the copolymer increased from 12 to 19 mol % or 11 to 22 mol %, respectively. This effect of benzannelation is also reflected by the copolymerization parameters. Both r_E and r_O are very similar for I and MI or BI and MBI, respectively.

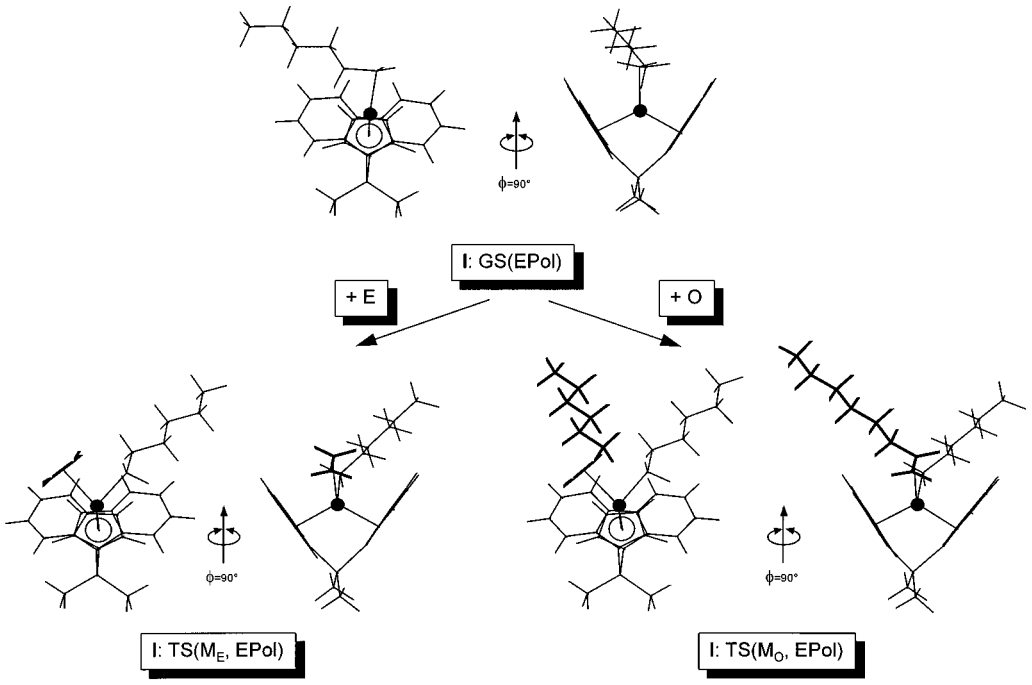

Figure 4. Structures of ground (GS) and transition (TS) states determined by force field calculations (metallocene, I; last inserted monomer unit, ethene).

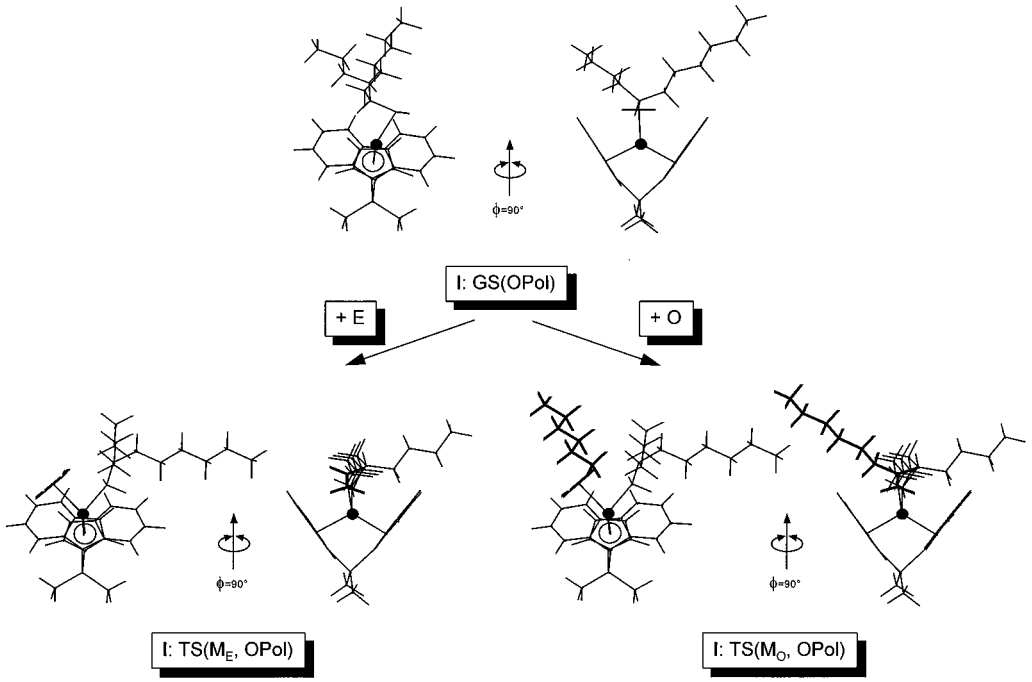

Figure 5. Structures of ground (GS) and transition (TS) states determined by force field calculations (metallocene, I; last inserted monomer unit, 1-octene).

Table 5. Monomer Sequence Distributions Determined by ^{13}C-NMR[a,b]

	metallocene (run no.)				
	I (1)	MI (2)	BI (3)	MBI (4)	MBI (6)
T_{EOE}[a,b]	0.109 (0.107)	0.103 (0.105)	0.130 (0.135)	0.128 (0.125)	0.094 (0.088)
$T_{EOO+OOE}$	0.008 (0.008)	0.005 (0.007)	0.055 (0.056)	0.080 (0.081)	0.029 (0.027)
T_{OOO}	0.001 (0.000)	0.002 (0.000)	0.005 (0.006)	0.015 (0.013)	0.001 (0.002)
T_{OEO}	0.019 (0.014)	0.019 (0.013)	0.032 (0.033)	0.039 (0.035)	0.017 (0.012)
$T_{OEE+EEO}$	0.190 (0.195)	0.190 (0.191)	0.268 (0.260)	0.255 (0.261)	0.169 0.179
T_{EEE}	0.673 (0.675)	0.681 (0.683)	0.510 (0.509)	0.483 (0.485)	0.690 (0.692)
deviation[c]	1.0×10^{-5}	0.8×10^{-5}	1.4×10^{-5}	1.1×10^{-5}	3.1×10^{-5}

[a] T_{EEE}, $T_{EEO+OEE}$, T_{EOE}, $T_{EOO+OOE}$, T_{OEO}, T_{OOO} = triad distribution determined by using the method described by *Randall*.[19] [b] Values in parentheses are simulated using first-order Markov statistics. [c] Deviation is calculated using the following equation: deviation = $[\sum(T_{NMR} - T_{Markov})^2]/n$ (T_{NMR} = triads determined by NMR, T_{Markov} = simulated triads, n = number of triads[6]).

Table 6. Results of the Force Field Calculations

	metallocene			
	I	MI	BI	MBI
E_{GS}(E-Pol) (kJ/mol)	261.3	248.9	546.8	536.8
E_{TS}(M$_E$, E-Pol) (kJ/mol)	298.9	286.2	587.1	576.1
E_{TS}(M$_O$, E-Pol) (kJ/mol)	313.3	301.0	599.1	589.5
E_a(M$_E$, E-Pol) (kJ/mol) = E_{TS}(M$_E$, E-Pol) − (E_{GS}(E-Pol) + E_E)	37.8	37.5	40.5	39.4
E_a(M$_O$, E-Pol) (kJ/mol) = E_{TS}(M$_O$, E-Pol) − (E_{GS}(E-Pol) + E_O)	51.6	51.7	51.9	52.3
E_a(M$_O$, E-Pol) − E_a(M$_E$, E-Pol) (kJ/mol)	13.9	14.2	11.4	12.8
E_{GS}(O-Pol) (kJ/mol)	267.4	256.6	554.5	545.4
E_{TS}(M$_E$, O-Pol) (kJ/mol)	316.5	305.3	598.8	586.8
E_{TS}(M$_O$, O-Pol) (kJ/mol)	333.2	323.7	614.0	603.1
E_a(M$_E$, O-Pol) (kJ/mol) = E_{TS}(M$_E$, O-Pol) − (E_{GS}(O-Pol) + E_E)	49.2	48.9	44.5	41.5
E_a(M$_O$, O-Pol) (kJ/mol) = E_{TS}(M$_O$, O-Pol) − (E_{GS}(O-Pol) + E_O)	65.4	66.7	59.1	57.3
E_a(M$_O$, O-Pol) − E_a(M$_E$, O-Pol) (kJ/mol)	16.2	17.8	14.6	15.7
E_a(M$_E$, O-Pol) − E_a(M$_E$, E-Pol) (kJ/mol)	11.5	11.4	4.1	2.1
E_a(M$_O$, O-Pol) − E_a(M$_O$, E-Pol) (kJ/mol)	13.8	15.1	7.2	5.0

[a] E_{GS} = calculated energy of ground state (see Figure 1 and Table 1), E_{TS} = calculated energy of transition state (see Figure 1 and Table 2), E_a = calculated energy differences between ground and transition states, E_E = calculated ground state energy of ethene (−0.2 kJ/mol), E_O = calculated ground state energy of 1-octene (+0.4 kJ/mol).

Benzannelation, in contrast to 2-methyl substitution, however, significantly changed the copolymerization parameters, increasing r_O and decreasing r_E. Moreover, only in the case of benzannelation does $r_E r_O$ approach 1, as expected for random 1-octene incorporation. In conclusion, 2-methyl substitution favors molecular mass buildup, whereas benzannelation promotes higher 1-octene incorporation and random distribution of 1-hexyl short-chain branches, resulting from 1-octene incorporation, along the polyethylene chain. As expected, higher 1-octene content correlates with lower glass transition temperatures of the resulting poly(ethene-*co*-1-octene) which was found to be −59 °C for poly(ethene-*co*-1-octene), containing 22 mol % 1-octene.

As summarized in Table 4, MAO-activated *rac*-Me_2Si[2-Me-Benz[*e*]Ind]$_2ZrCl_2$ was used to homo- and copolymerize ethene and 1-octene with variation of the 1-octene content: 0, 60, 75, and 100 mol %. Both catalyst activity and copolymer molecular mass decrease substantially when the content of the less reactive, sterically hindered 1-octene is increased.

Copolymerization parameters, determined at 25 and 40 mol % ethene content were found to be identical and independent of the ethene/1-octene molar ratio. Similar to results reported above, increasing the 1-octene content at 1-octene molar content higher than 60 mol % decreased the glass transition temperature of the resulting copolymers to approach the value of poly(1-octene). The decrease of the number average molecular mass with an increase of the 1-octene content in the monomer feed as well as in the poly(ethene-*co*-1-octene) copolymer is shown in Figure 3.

Analysis of the triad distribution, measured by means of ^{13}C-NMR spectroscopy, and summarized in Table 5, clearly confirms that copolymerization of ethene with 1-octene follows first-order Markov statistics. Additional evidence for the validity of first-order Markov statistics represents the result that *r* parameters, calculated from the diad distribution, are independent of monomer concentration.

To investigate the reasons concerning the effect of benzannelation on ethene copolymerization, force field calculations (Biosym Software: forcefield Discover) were applied to calculate the difference of activation energy for inserting ethene or 1-octene, respectively. The transition state of this insertion reaction, involving cationic zirconcene intermediate, is displayed in Figure 1. The calculation procedure is discribed in the Experimental Section.

The calculated energy values of the ground and transition states cannot be used for discussing experimental data, because force field calculations do not include electronic effects. But energy differences between similar molecules show the differences in steric hindrance. Table 6 summarizes the results of the force field calculations and calculated energy differences. The calculated activation energies show that an insertion of 1-octene has more steric hindrance compared with an insertion of ethene ($E_a(M_O$, E-Pol) > $E_a(M_E$, E-Pol) and $E_a(M_O$, O-Pol) > $E_a(M_E$, O-Pol)). Thus, insertion of an ethene monomer is preferred compared with insertion of a 1-octene monomer. The differences of these activation energies ($E_a(M_O$ E-Pol) − $E_a(M_E$, E-Pol) and $E_a(M_O$, O-Pol) − $E_a(M_E$, O-Pol)) are lower in the case of the benzannelated metallocenes (BI and MBI) compared with the corresponding metallocenes without benzannelation (I and MI). Therefore, benzannelated metallocenes have a higher tendency to incorporate 1-octene. This result confirms the experimental data of 1-octene incorporation and *r* parameters (see Table 3). Moreover, comparisons of differences of activation energies with the same coordinated monomer but different last inserted monomer units in the polymer chain ($E_a(M_E$, O-Pol) − $E_a(M_E$, E-Pol) and $E_a(M_O$, O-Pol) − $E_a(M_O$, E-Pol)) also show lower values in the case of the benzannelated metallocenes (BI and MBI) compared with the corresponding metallocenes without benzannelation (I and MI). In the case of the benzannelated metallocenes, the last inserted monomer unit in the polymer chain has a weaker impact on the insertion of the next monomer unit. Benzannelated metallocenes show a more random distribution of the monomers in the polymer chain ($r_E r_O \approx 1$) compared with the metallocenes without benzannelation ($r_E r_O \approx 0.3$), which results from the different activation energies as calculated above.

Conclusion

Stereoselectivity and comonomer incorporation of metallocene-catalyzed polymerization are dependent on metallocene type and structure, especially the indenyl ligand substitution pattern. In the $Me_2Si(Ind)_2ZrCl_2$ family, benzannelation substantially improves comonomer incorporation and randomness of comonomer incorporation, whereas 2-methyl substitution promotes a high degree of polymerization. 2-Methyl substitution appears to prevent chain transfer to monomer, which would result fom β-hydride transfer from the last monomeric unit of the polymer chain to the monomer.[10,11] Although mechanistic aspects of benzannelation are not very well understood, relative activation energies for ethene and 1-octene insertion, which result from forcefield calculations, and the experimental data show that benzannelation enhances incorporation of higher 1-olefins with respect to ethene.

Acknowledgment. The authors gratefully acknowledge support by the Bundesminister für Forschung und Technologie (project no. 03M40719) and by BASF AG. Also the authors would like to thank Prof. Dr. H.-H. Brintzinger and his group for supplying us with metallocene complexes and for many stimulating discussions. J.S. is grateful for a fellowship by the Studienstiftung des Deutschen Volkes.

References and Notes

(1) Aulbach, M.; Küber, F. *Chem. Z.* **1994**, *28*, 197.
(2) Huang, J.; Rempel, G. L. *Prog. Polym. Sci.* **1995**, *20*, 459.
(3) Brintzinger, H. H.; Fischer, D.; Mülhaupt, R.; Rieger, B.; Waymouth, R. *Angew. Chem.* **1995**, *107*, 1255.
(4) Herfert, N.; Montag, P.; Fink, G. *Makromol. Chem.* **1993**, *194*, 3167.
(5) Mühlenbrock, P. H.; Fink, G. *Z. Naturforsch.* **1995**, *50B*, 423.
(6) Koivumäki, J.; Seppälä, J. V. *Macromolecules* **1993**, *26*, 5535.
(7) Koivumäki, J.; Fink, G.; Seppälä, J. V. *Macromolecules* **1994**, *27*, 6254.
(8) Koivumäki, J.; Seppälä, J. V. *Polymer* **1993**, *34*, 1958.
(9) (a) Batistini, A. *Macromol. Symp.* **1995**, *100*, 137; (b) Bensason, S.; Minick, J.; Moet, A.; Chum, S.; Hiltner, A.; Baer, E. *J. Polym. Sci., Part B* **1996**, *34*, 1301.
(10) Stehling, U.; Diebold, J.; Kirsten, R.; Röll, W.; Brintzinger, H. H.; Jüngling, S.; Mülhaupt, R.; Langhauser, F. *Organometallics* **1994**, *13*, 965.
(11) Spaleck, W.; Antberg, M.; Rohrmann, J.; Winter, A.; Bachmann, B.; Kiprof, P.; Behm, J.; Herrmann, W. A. *Angew. Chem.* **1992**, *104*, 1373.
(12) Spaleck, W.; Küber, F.; Winter, A.; Rohrmann, J.; Bachmann, B.; Antberg, M.; Dolle, V.; Paulus, E. F. *Organometallics* **1994**, *13*, 954.
(13) Spaleck, W.; Antberg, M.; Dolle, V.; Klein, R.; Rohrmann, J.; Winter, A. *New J. Chem.* **1990**, *14*, 499.
(14) Soga, K. *Makromol. Chem., Macromol. Symp.* **1993**, *66*, 43.
(15) Uozumi, T.; Soga, K. *Makromol. Chem.* **1992**, *193*, 823.
(16) Zambelli, A.; Grassi, A. *Makromol. Chem., Rapid Commun.* **1991**, *12*, 523.
(17) Tsai, W.-M.; Chien, J. C. W. *J. Polym. Sci., Part A* **1994**, *32*, 149.
(18) Chien, J. C. W.; Nozaki, T. *J. Polym. Sci., Part A* **1993**, *31*, 227.
(19) Randall, J. C. *J. Macromol. Sc., Rev. Macromol. Chem. Phys.* **1989,** *C29*, 201.
(20) Jordan, R. F.; Bradley, P. K.; Baenzinger, N. C.; LaPointe, R. E. *J. Am. Chem. Soc.* **1990**, *112*, 1289.
(21) Woo, T. K.; Fan, L.; Ziegler, T. *Organometallics* **1194**, *13*, 2252.
(22) Prosenc, M. H. In *Diplomarbeit, Universität Konstanz,* **1993**.

MA961844Z